International Journal of Basic and Applied Biology
p-ISSN: 2394-5820, e-ISSN: 2349-2539, Volume 3, Issue 2; April-June, 2016, pp. 104-110

http://www.krishisanskriti.org/Publication.html

Designing of *Plasmodium Falciparum* Leucyl Aminopeptidase Inhibitors for Substrate Ingress/Egress Path Using Virtual Screening

Meenakshi Chaudhary[1] and Shakti Sahi[2]*

[1,2]School of Biotechnology, Gautam Buddha University, Greater Noida, India-20130
E-mail: [1]nain.meenakshi@gmail.com, [2]shaktis@gbu.ac.in

Abstract—*Plasmodium falciparum leucyl aminopeptidase (PfA-M17) is an attractive anti-malarial drug target. Discovery of PfA-M17 inhibitors has been focused on targeting the active site. Non-specificity and off target activity of known aminopeptidase inhibitors limit their use as an antimalarial drug.Therefore, identifying new PfA-M17 inhibitors which function through a different mechanism could complement current drug design strategies and improve drug efficacy. In this study, we explored a novel binding site of PfA-M17 and identified new PfA-M17 inhibitors through receptor based virtual screening. A library of 244,839 compounds were screened using receptor-based virtual screening against the predicted cavity of PfA-M17, and three levels of accuracy were used: high-throughput virtual screening, grid-based ligand docking with energetics (Glide) standard precision and Glide extra precision. Our findings reveal a new drug targeting site for malaria therapy.*

1. INTRODUCTION

Plasmodium falciparum is responsible for the majority of malaria infections worldwide, resulting in over a million deaths annually [1]. Malaria parasites now show measured resistance to all currently utilized drugs [2, 3]. Novel antimalarial drugs are urgently needed. The *Pf*A-M17 is a novel target for the development of innovative antimalarials [4, 5]. We recently described the first potent *Pf*A-M17 alosteric site inhibitor of the enzyme (communicated). The identification of allosteric sites in proteins, that prefer therapeutic agents over classic orthosteric ligands (higher specificity, fewer side effects and lower toxicity) [6]. An advantage of targeting substrate ingress/egress sites for therapeutic interaction is a reduced risk of secondary adverse effects. This is because substrate ingress/egress sites appear to be significantly less conserved than active sites across homolog proteins, enabling the design of drugs with high specificity for a single protein within a protein family. It is expected that a deeper understanding of the properties of substrate ingress/egress sites and their identification with ligands would help streamlining the design and discovery of novel therapeutic drugs [7] and (Fig. 1d).

In continuation of our efforts towards the definition of the regulatory and substrate ingress/egress site inhibitor interaction, we herein propose the first comprehensive computational investigation of the *Pf*A-M17 using molecular docking approaches. Investigation of the differences in the binding sites as well as the interactions of our inhibitors with *Pf*A-M17, allowed us to highlight the structurally relevant regions of the enzyme that could be targeted for developing *Pf*A-M17 inhibitors. We have discovered few novel compounds that could be selectively inhibit the *Pf*A-M17 activity and could be the great potential as anti malarial drug candidates. This study was validated by applying in silico methods, showing that it may be useful for the future development of potent antimalarial agents.

2. MATERIAL AND METHODS

2.1. Receptor-based virtual screening

2.1.1 Protein preparation and grid generation

The co-ordinates of *Pf*A-M17 at 2.4 Å resolution (PDB ID: 3KQZ) were retrieved from the Protein Data Bank (PDB). Monomer (Chain: A) of the *Pf*A-M17 was used for receptor based virtual screening. Prior to docking, the *Pf*A-M17 protein was prepared using Maestro v 9.7 [8] by assigning bond orders and addition of hydrogen atoms. Further, addition of missing side chains & missing atoms using Schrodinger’s Prime 3.5 [9] and Hydrogen bonding network was optimized by predicting tautomeric and ionization states [10]. Receptor binding site was defined by grid generation using Glide [11]. The docked length of outer box and inner box size were same 47x47x47Å and 38x38x38 Å each respectively.

3. LIGAND PREPARATION

An in-house database of small molecules of both natural and synthetic origin was constructed from various libraries Ligand.Info [12] Druglikeness [12], Chembank [12], Not annotated NCI [12],Oxime [13] Zinc [14], DrugBank [15] and Schrödinger [16] (Fig. 1a). The Ligands were prepared with ligprep [17] and Epik [10]. The physicochemically significant descriptors and pharmacokinetically relevant properties which includes absorption, distribution, metabolism, and excretion (ADME) properties were taken into consideration [18] in supplementary material. Pre-filtration was done using Lipinski's rule of five [19].

The structure based virtual screening was done in three phases namely, HTVS (High Throughput Virtual Screening), SP (Standard-Precision) and XP (Extra-Precision) using Glide (Fig. 1a).

4. RESULTS AND DISCUSSION

4.1 Receptor-based Virtual Screening

A total of 244,830 compounds were screened according to a stepwise filtering protocol. Compounds with high molecular weight (MW >500) and with reactive functional groups were eliminated, and the remaining compounds were docked into the predicted site of the *Pf*A-M17. In the first stage of screening, the compounds were docked with Glide HTVS. A total of 167,226 hits were obtained and ranked according to the G-Score. These hits were further refined by re-docking them using Glide SP; 222,428 hits were then retained. These surviving hits were passed onto the third stage XP docking a total of 2,095 hits were kept for further analysis (Fig. 1b**).** In the end 30 compounds were selected those docking score was -8.30 to -7.0 (kcal/mol) (Fig. 1c).

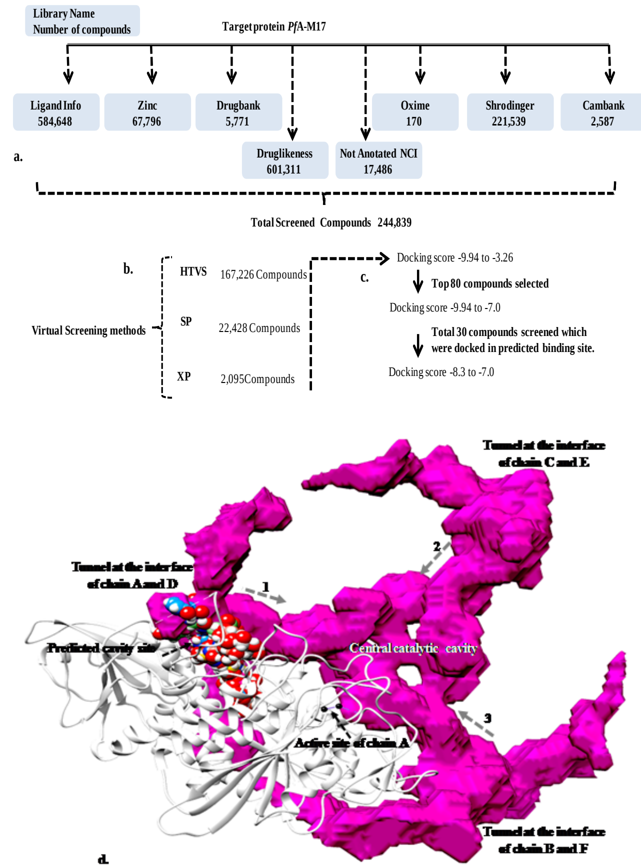

Fig. 1a, b and c: A flow chart depicting protocol for receptor based virtual screening. **Fig. 1d:** All major channels in the ligand unbound structure of *Pf*A-M17. For clarity only chain A of the hexamer is shown here. The ligands docked in *Pf*A-M17 Chain A in potential predicted cavity are shown in colored sphere and three major tunnels (1-3) pass through the interface of two oppositely oriented chains (A-D, C-E or B-F) merge in the center to form central catalytic cavity.

Table 1: Interaction energies and distance between the ligand and key amino acids of *Pf*A-M17 in glide XP docking complex determined using LIGPLOT program.

Compound Number	M W	Docking Score	Glide Energy	Hydrogen bond interections	Hydrophobic interections
Compound 1	300	-8.3	-15.7	S-Asn582(ND2-2.9-O2)L.	Lys204,Leu208,Tyr244,Glu245,Ala585,Lys589,Arg594.
Compound 2	135	-8.0	-24.6	S-Arg594(NH2-2.89-N3)L.	Lys204,Thr241,Thr244,Glu245,Lys589,Phe591.
Compound 3	395	-8.0	-38.3	S-Asn582(ND2-3.04-O3)L, S-Ser295(OG-2.78-F1)L.	Lys208,Thr244,Glu245,Met247,Thr248,Asp249,Ala584,Ala585,Lys587.
Compound 4	155	-7.8	-20.1	S-Glu245(OE3-2.53-N2)L, S-Glu245(OE3-3.09-N3)L, S-Asn582(ND2-2.95-O1)L, S-Lys204(NZ-2.58-N1)L, S-Lys204(NZ-3.0-O1)L, S-Arg594(NB2-2.84-N5)L.	Thr241,Tyr244,Lys589.

Compound 5	367	-7.8	-42.1	B-Glu240(O-3.13-O1)L, S-Thr(OG1-2.65-O2)L, S-Arg594(NB2-2.66-O2)L, S-Arg594(NB1-2.75-O2)L, B-Lys589(O-2.8-O3)L, S-Lys204(NZ-2.893.0-O6)L.	Lys208,Phe237,Tyr244,Thr291,Asn582,Ala584.
Compound 6	273	-7.6	-34.5	S-Thr241(OC1-2.86-O1)L, S-Lys204(NZ-2.66-O6)L, S-Lys204(NZ-2.85-O3)L, S-Arg594(NB1-3.31-O1)L, S-Arg594(NB2-2.95-O4)L, S-Arg594(NB2-2.89-O1)L.	Lys208,Phe237,Tyr244,Glu245,Thr291,Asn582.
Compound 7	300	-7.6	-45.0	B-Glu245(O-2.65-O1)L, S-Lys587(NZ-3.26-O3)L.	Met247,Thr248,Asn249,Thr292,Ser295,Ala585.
Compound 8	416	-7.5	-47.1	NO	Asn216,Tyr246,Glu262,Tyr263,His215,Thr248,Met247,Lys587,Asp249,Lys253,Glu250.
Compound 9	370	-7.5	-40.9	B-Phe583(N-3.22-O5)L, S-Lys584(NZ-2.94-O1)L, S-Lys589(N2-3.06-O3)L, S-Lys204(NZ-2.94-O3)L, S-Arg205(NL-2.82-O1)L, S-Arg205(NQ2-2.70-O1)L.	Ala585,Asn582,Leu208,Thr497.
Compound 10	201	-7.5	-25.8	B-Glu245(OE2-2.62-O1)L, B-Glu245(OE2-2.38-N1)L, S-Asn582(ND2-2.78-O2)L. S-Lys204(NZ-2.48-O3)L,	Glu200,Tyr244,Phe237,Phe591,Glu522,Asn521,Pro523,Arg594,Lys589.
Compound 11	448	-7.5	-42.2	S-Lys589(NZ-3.04-O2)L, S-Lys204(NZ-2.86-O1)L, S-Asn582(ND2-2.88-O9)L, S-Arg205(NE-2.99-O1)L, S-Arg205(NB2-2.88-O1)L.	Leu208,Glu245,Lys587.
Compound 12	187	-7.4	-31.0	S-Lys204(NZ-2.7-O3)L, S-Arg594(NB1-2.92-O1)L, S-Arg594(NB2-2.83-O1)L, S-Thr241(OG1-2.87-O1)L.	Tyr244,Glu240,Thr291,Glu245,Lys589.
Compound 13	243	-7.4	-33.1	S-Arg205(NH1-2.83-O2)L, S-Arg205(NE-2.96-O2)L, S-Lys584(NZ-2.78-O1)L, B-Phe583(N-2.92-O4)L, S-Thr497(OG1-2.8-N5)L, S-Ser498(OG-3.21-O5)L.	Asn582,Lys589.
Compound 14	201	-7.4	-30.4	S-Lys204(NZ-2.76-O1)L, S-Lys204(NZ-2.46-O3)L, S-Glu245(OE2-2.79-N1)L, S-Asn582(ND2-2.70-O2)L.	Tyr244,Phe591,Pro523,Glu200,Lys589,Phe237,Arg594.
Compound 15	474	-7.4	-55.9	S-Thr248(OG1-2.74-O1)L, B-Arg586(O-3.13-O1)L, S-Lys397(NZ-2.84-O4)L.	Ala585,Val211,His215,Thr212,Leu208,Lys587,Tyr292,Ser295,Glu245,Ala299,Asp249,Pro588.
Compound 16	372	-7.4	-19.6	S-Lys589(NZ-3.11-O1)L, S-Lys589(NZ-2.99-O2)L, S-Lys204(NZ-2.68-N3)L.	Asn582,Lys584,Leu208,ARG594,Glu245,Thr291,Glu240, Tyr244,Thr241.
Compound 17	492	-7.3	-50.5	S-Glu245(OE1-3.14-N3)L, S-Ser498(OG-2.89-O2)L.	Thr248,His215,Leu208,Arg205,Lys584,Ala201,Lys598,Lys204,Ala585,Asn582.
Compound 18	113	-7.3	-30.1	S-Arg594(NB2-2.78-O1)L, S-Arg594(NB1-3.22-O1)L, S-Lys204(NZ-3.03-N3)L, S-Asn582(ND2-2.86-O2)L, S-Glu245(OE2-2.52-N1)L.	Phe237,Thr241,Tyr244,Lys589.

Compound 19	332	-7.3	-43.9	S-Arg594(NH2-2.87-O2)L, S-Arg594(NH2-2.73-O1)L, S-Lys204(NZ-2.89-O6)L, S-Glu245(OE2-2.61-O5)L, S-Glu245(OE2-2.76-N1)L.	Asn582,Lys584,Leu208,Thr241,Tyr244.
Compound 20	363	-7.2	-37.2	S-Asp216(OD1-3.2-N1)L, S-Asp216(OD1-2.65-N5)L, S-Asp216(OD2-2.6-N4)L.	Thr248,Leu214,His215,Leu208,Glu245,Thr212.
Compound 21	291	-7.2	-31.4	S-Lys584(NZ-2.86-N1)L, S-Lys589(NZ-3.01-O3)L, S-Ser498(OG-3.33-N3)L, S-Arg205(NE-3.15-O3)L.	Leu208,Lys204.
Compound 22	160	-7.2	-22.9	S-Arg594(NH2-2.79-O1)L, S-Glu245(OE2-2.69-N2)L, B-Tyr287(O-2.94-N1)L.	Glu240,Tyr288,Thr291,Thr241,Tyr244,Lys589,Lys204.
Compound 23	196	-7.1	-34.8	S-Glu200(OE2-2.9-O1)L, S-Lys204(NZ-2.77-O1)L, S-Lys204(NZ-2.86-O2)L, S-Lys204(NZ-2.68-O7)L, S-Asn582(ND2-3.0-O6)L, S-Glu245(OE2-2.81-O5)L, B-Lys589(O-2.92-O3)L.	Pro523,Thr241,Phe237,Arg594,Tyr244,Phe591.
Compound 24	179	-7.1	-27.5	S-Lys204(NZ-3.11-O1)L, S-Glu245(OE3-2.63-N1)L, S-Thr241(OG1-2.85-O3)L, S-Arg594(NH2-2.90-O2)L, S-Arg594(NH1-3.23-O3)L.	Lys589,Glu522,Phe237,Tyr244,Asn582.
Compound 25	153	-7.1	-23.1	S-Lys204(NZ-2.68-O3)L, S-Glu245(OE2-2.87-N1)L, S-Asn582(ND2-2.67-O2)L.	Arg594,Tyr244,Lys589.
Compound 26	300	-7.1	-44.1	B-Arg586(O-3.03-N1)L, S-Lys587(NZ-3.23-O3)L, B-Met247(O-2.95-O3)L, B-Tyr244(O-3.08-O2)L, B-Asp249(O-2.79-O1)L.	Phe252,Glu250,Ser295,Thr248,Tyr292.
Compound 27	167	-7.1	-26.8	S-Lys204(NZ-2.45-O3)L, S-Asn582(ND2-2.71-O2)L, S-Glu245(OE2-2.78-N1)L.	Arg594,Tyr244,Lys589,Asn521,Pro523,Glu522,Glu200.
Compound 28	291	-7.1	-26.3	S-Lys204(NZ-2.80-O1)L, S-Glu245(OE2-2.56-N1)L, S-Asn582(ND2-2.66-O2)L.	Thr241,Arg594,Thr291,Tyr244,Lys589,Leu208,Ala585,Lys584.
Compound 29	398	-7.0	-40.1	S-Thr248(OG1-2.96-N2)L, S-Thr248(OG1-3.23-N3)L, S-Glu250(OE2-2.91-N1)L.	Asp249,Asp299,Pro588,Lys587,Ser295,Met245,Tyr244,Tyr292.
Compound 30	321	-7.0	-38.6	S-Lys253(NZ-3.04-O4)L, S-Arg586(NH2-3.11-O5)L.	Met247,Tyr292,Tyr244,Ser295,Asp249,Pro588,Ala299,Lys587.

Abbreviation: S- side chain, B- backbone - Residue name with number (atom-H bond distance in Å -ligand atom with number) L- ligand.

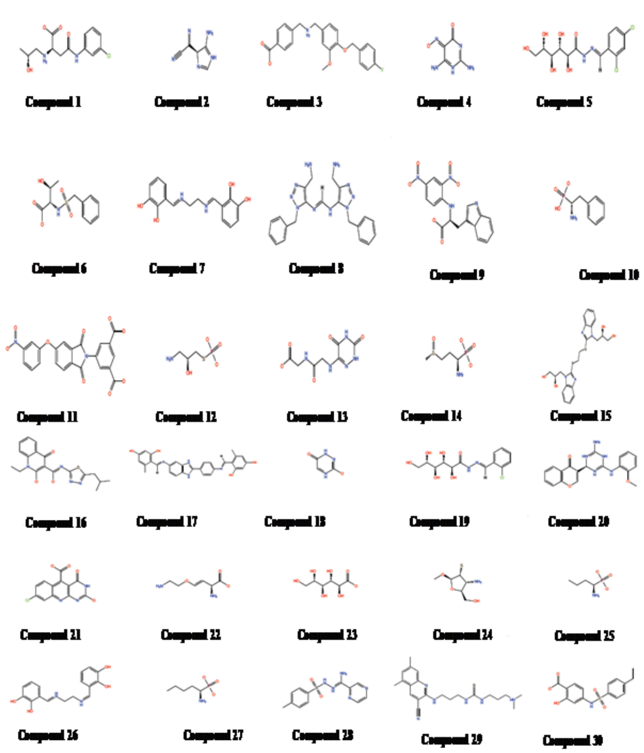

Fig. 2: 2 D structure of 30 potential inhibitors of the *Pf*A-M17 enzyme.

5. POST DOCKING ANALYSIS

On the basis of the docking score, ligand receptor interaction, stereochemical considerations and energetics of the docked complex top 80 compounds were selected (Fig. 1c). The docked complexes were analyzed on the basis of their docking site; finally 30 compounds were selected (Fig. 1c and Fig. 2). Values of drug like properties of these compounds were consistent with the guidelines for selecting orally available drug-like molecules [20], and with the acceptable range of Lipinski's rule of five [19] (supplementary data Table S1).

The primary observations of the ligand interactions with the receptor showed that coordinating atoms (N/O) of 8 compounds (compounds 4,10,14,18,19,20,27 and 28) and receptor were placed within a strong coordinating distance (< 2.6 Å) (Table 1). The side chain oxygen of Glu245 formed hydrogen bond interaction with distance < 2.6 Å with all above said compounds except compound 20 (Table 1). The compound 4, 10, 14 and 27 also formed hydrogen bond with The Lys204 oxygen with distance < 2.5 Å (Table 1).

These compounds also formed hydrophobic interactions with receptor residues and stabilized the ligand in the cavity. Some important residues such as Leu208, Tyr244 and Lys589 formed hydrophobic interactions with 3 compounds 1, 19 and 28. These residues are important because they involved in interchain interaction. Other compounds interacted with either 2 or 1 of these 3 residues except compounds 7-8 and 26 (table 1). Only Compound 20 that interact differently as compare to other compounds, formed hydrogen bond and hydrophobic interaction with Asp216 and His215 respectively. This His215 is involved in N-terminal domain inter chain interaction with Lys173, such as chain A and chain D respectively.

From the observations in the present study, further, ligand binding in substrate ingress/egress site may be evaluated by X-ray crystallography.

6. CONCLUSION

A loop region ~20 Å between helix 3 and strand 6 sits at the entrance to the catalytic cavity, play a key role in the control of substrate excess to central catalytic cavity [5]. This loop forms contacts with residues of the N- and C- terminal domains and control access to the catalytic cleft. The reorientation of the loop and opening of the catalytic cleft are thought to be required during the allosteric transition to allow substrate to bind at the active site, hence referred to as the active site gate.

In the present study 244,839 compounds were screened computationally to reduce time and resource for bioassay screening. We identified 30 compounds that bind at the gated opening of the active site. Out of 30 compound 8 compounds were selected on the basis of receptor ligand interaction studies. Binding of ligands at gated opening of active site that either change the flexibility of loop or create steric hindrance in the channel connecting opening to the active site, can be lead to inhibition of enzyme activity. These potential *Pf*A-M17 inhibitors will be further evaluated in *Pf*A-M17 enzyme inhibition assay.

7. ACKNOWLEDGMENTS

The authors gratefully acknowledge the support of this work by the Department of Biotechnology (DBT), Ministry of Science and Technology, Government of India.

8. CONFLICTS OF INTEREST

The authors declare no conflict of interest.

REFERENCES

[1] World Health Organization,World Malaria Report ,Geneva. 2015.
[2] Costanzo, M.S., Hartl, D.L. The evolutionary landscape of antifolate resistance in Plasmodium falciparum. J Genet. 2011, 90, 187-190.
[3] Ariey, F., Witkowski, B., Amaratunga, C., Beghain, J., Langlois, A.C., Khim, N., et al. A molecular marker of artemisinin-resistant Plasmodium falciparum malaria. Nature. 2014, 505, 50-55.
[4] Gardiner, D.L., Skinner-Adams, T.S., Brown, C.L., Andrews, K.T., Stack, C.M., McCarthy, J.S., et al. Plasmodium falciparum: new molecular targets with potential for antimalarial drug development. Expert Rev Anti Infect Ther. 2009, 7, 1087-1098.
[5] McGowan, S., Oellig, C.A., Birru, W.A., Caradoc-Davies, T.T., Stack, C.M., Lowther, J., et al. Structure of the Plasmodium falciparum M17 aminopeptidase and significance for the design

of drugs targeting the neutral exopeptidases. Proc Natl Acad Sci U S A. 2010, 107, 2449-2454.
[6] Nussinov, R.T., C. J. Allostery in disease and in drug discovery. Cell. 2013, 153, 293-305.
[7] Kholodar, S.A., Tombline, G., Liu, J., Tan, Z., Allen, C.L., Gulick, A.M., et al. Alteration of the flexible loop in 1-deoxy-D-xylulose-5-phosphate reductoisomerase boosts enthalpy-driven inhibition by fosmidomycin. Biochemistry. 2014, 53, 3423-3431.
[8] Maestro, 9.7,Schrödinger, LLC,New York,NY,USA. 2014.
[9] Prime,3.5, Schrödinger, LLC,New York,NY,USA. 2014.
[10] Epik,2.7, Schrödinger,LLC,New York,NY,USA. 2014.
[11] Glide, Version 6.2, Schrödinger, LLC, New York, NY. 2014.
[12] von Grotthuss, M., Koczyk, G., Pas, J., Wyrwicz, L.S., Rychlewski, L. Ligand.Info small-molecule Meta-Database. Comb Chem High Throughput Screen. 2004, 7, 757-761.
[13] Babu, P.A., Puppala, S.S., Aswini, S.L., Vani, M.R., Kumar, C.N., Prasanna, T. A database of natural products and chemical entities from marine habitat. Bioinformation. 2008, 3, 142-143.
[14] Irwin, J.J., Shoichet, B.K. ZINC--a free database of commercially available compounds for virtual screening. J Chem Inf Model. 2005, 45, 177-182.
[15] Wishart, D.S., Knox, C., Guo, A.C., Shrivastava, S., Hassanali, M., Stothard, P., et al. DrugBank: a comprehensive resource for in silico drug discovery and exploration. Nucleic Acids Res. 2006, 34, D668-672.
[16] Schrödinger, LLC, New York, NY, www.schrodinger.com. 2010.
[17] LigPrep, 2.9, Schrödinger, LLC,New York,NY,USA. 2014.
[18] QikProp, 3.9, Schrödinger, LLC,New York,NY,USA. 2014.
[19] Lipinski, C.A., Lombardo, F., Dominy, B.W., Feeney, P.J. Experimental and computational approaches to estimate solubility and permeability in drug discovery and development settings. Adv Drug Deliv Rev. 2001, 46, 3-26.
[20] Oyelere, A.K. Macrocycles in medicinal chemistry and drug discovery. Curr Top Med Chem. 2010, 10, 1359-1360.

Supplementary Data TableS1: Drug like properties of the selected compounds

Compound Name	QPpolrz	QPlogPC16	QPlogPoct	QPlogPw	QPlogPo/w	QPlogS	CIQPlogS	QPlogBB	QPlogKp	QPlogKhsa	%Human Oral Absorption	PSA
Compound 1	28.9	10.6	17.7	12.6	-0.3	-2.9	-2.0	-1.0	-5.4	-0.6	46.4	114.9
Compound 2	11.2	5.6	11.5	11.9	-1.5	-1.5	-1.7	-1.4	-5.2	-0.9	50.6	102.9
Compound 3	43.5	14.1	20.1	10.9	3.0	-6.1	-5.2	-0.8	-3.5	0.5	75.1	77.0
Compound 4	10.2	6.1	15.0	15.0	-2.0	-0.5	-1.0	-1.9	-6.0	-0.9	39.4	127.9
Compound 5	28.9	12.6	23.8	18.1	0.4	-2.8	-3.1	-2.3	-4.0	-0.9	49.3	144.2
Compound 6	25.0	9.1	13.9	10.3	1.7	-2.7	-2.6	-1.7	-4.0	-0.7	62.2	117.6
Compound 7	30.1	11.9	19.0	13.8	1.8	-3.1	-3.5	-2.0	-2.8	-0.4	77.8	103.0
Compound 8	40.3	14.7	25.7	17.0	1.4	-0.9	-3.6	-1.2	-7.5	0.0	48.5	148.1
Compound 9	29.1	11.1	18.8	11.7	1.5	-2.0	-5.0	-1.7	-4.9	-0.4	53.7	153.2
Compound 10	17.3	7.7	15.3	13.4	-1.5	-0.4	-0.5	-0.6	-5.4	-1.1	30.0	84.9
Compound 11	43.1	15.2	24.3	16.4	2.0	-5.2	-6.2	-3.9	-7.3	-0.2	8.7	210.2
Compound 12	11.6	6.6	16.0	15.4	-3.1	-0.2	0.3	-1.4	-7.3	-1.4	6.9	111.8
Compound 13	18.9	8.0	16.2	16.1	-1.6	-0.6	-1.4	-2.8	-7.6	-1.2	13.2	200.8
Compound 14	14.2	6.6	16.7	18.8	-3.2	1.0	0.7	-1.2	-6.9	-1.4	0.0	105.8
Compound 15	45.4	17.0	26.3	17.6	3.0	-5.1	-5.9	-2.5	-2.5	-0.1	83.0	114.4
Compound 16	38.1	11.5	16.1	7.1	3.7	-5.3	-5.6	-1.3	-3.1	0.4	94.5	108.0
Compound 17	53.3	19.0	29.1	18.1	4.3	-7.2	-7.8	-2.9	-3.3	0.7	83.4	129.1
Compound 18	9.0	4.2	7.8	7.8	-0.8	-0.3	-1.0	-1.0	-5.0	-0.8	58.6	94.1

Compound 19	27.6	11.9	23.5	18.3	0.0	-2.2	-2.5	-2.4	-3.8	-1.0	46.7	144.2
Compound 20	38.6	12.9	22.8	16.4	2.4	-4.3	-5.0	-1.0	-2.3	0.0	89.4	104.9
Compound 21	24.8	9.3	17.1	13.9	0.6	-2.8	-3.4	-1.5	-5.3	-0.6	49.7	128.6
Compound 22	13.8	6.4	14.7	13.7	-3.6	0.9	1.3	-1.1	-9.1	-1.1	6.5	111.0
Compound 23	11.7	7.0	16.3	17.0	-1.8	-0.4	-0.5	-2.2	-5.6	-1.3	18.3	145.0
Compound 24	13.0	6.0	13.3	12.2	-0.8	0.3	0.2	0.1	-5.0	-0.8	65.5	64.5
Compound 25	11.3	5.4	12.9	12.2	-2.4	0.0	0.4	-0.8	-6.2	-1.2	22.9	85.2
Compound 26	30.4	11.6	17.8	12.8	1.7	-3.3	-3.5	-2.0	-3.1	-0.3	75.1	112.1
Compound 27	12.9	5.8	13.5	12.0	-2.1	-0.1	0.3	-0.9	-6.1	-1.3	24.5	85.3
Compound 28	27.8	10.2	17.8	13.9	0.8	-2.7	-3.1	-1.5	-3.7	-0.5	70.6	108.7
Compound 29	44.7	14.4	24.2	13.0	3.4	-6.4	-4.8	-1.2	-4.8	0.4	83.9	87.4
Compound 30	30.5	10.6	17.2	11.7	1.8	-3.3	-4.0	-2.0	-4.5	-0.3	58.8	117.9

Principal Descriptors Calculated for the selected Compounds: QPpolrz: Predicted polarizability in cubic angstroms. (Acceptable range: -13.0 – 70.0), QPlogPC16: Predicted hexadecane/gas partition coefficient. (Acceptable range: - 4.0 – 18.0), QPlogPoct: Predicted octanol/gas partition coefficient. (Acceptable range: 8.0 – 35.0), QPlogPw: Predicted water/gas partition coefficient. (acceptable range: -4.0 – 45.0), QPlogo/w: Predicted octanol/water partition co-efficient log p (acceptable range: -2.0 to 6.5), QPLogS : Predicted aqueous solubility; S in mol/L (acceptable range: -6.5 to 0.5), CIQPlogS : Conformation-independent predicted aqueous solubility, log S. S in mol dm–3 is the concentration of the solute in a saturated solution that is in equilibrium with the crystalline solid. (Acceptable range: –6.5 – 0.5), QPlogBB: Predicted brain/blood partition coefficient. Note: QikProp predictions are for orally delivered drugs so, for example, dopamine and serotonin are CNS negative because they are too polar to cross the blood-brain barrier (Acceptable range : –3.0 – 1.2), QPlogKp : Predicted skin permeability, log *K*p. (Acceptable range –8.0 to –1.0), QPlogKhsa: Prediction of binding to human serum albumin (Acceptable range: –1.5 – 1.5) , Percentage of human oral absorption (Acceptable range: <25% is poor and >80% is high) and PSA: Van der Waals surface area of polar nitrogen and oxygen atoms(Acceptable range 7.0 – 200.0).